

Low-temperature coherence in the periodic Anderson model: Predictions for photoemission of heavy Fermions

A. N. Tahvildar-Zadeh¹, M. Jarrell¹, and J. K. Freericks²

¹*Department of Physics, University of Cincinnati, Cincinnati, OH 45221-0011*

²*Department of Physics, Georgetown University, Washington, DC 20057-0995*

(August 14, 2018)

We present numerically exact predictions of the periodic and single-impurity Anderson models to address photoemission experiments on heavy Fermion systems. Unlike the single impurity model the lattice model is able to account for the enhanced intensity, dispersion, and apparent weak temperature dependence of the Kondo resonant peak seen in recent controversial photoemission experiments. We present a consistent interpretation of these results as a crossover from the impurity regime to an effective Hubbard model regime described by Nozieres.

Introduction Metallic compounds containing rare earth elements with partially filled f shells, such as CeBe₁₃ or UPt₃, belong to the general category of heavy fermions [1]. They are characterized by a large Pauli susceptibility and specific heat as compared to ordinary metals, which indicate a huge effective electronic mass, and also by anomalous transport properties such as non-monotonic temperature dependence of the resistivity. These anomalies are usually attributed to the formation of a resonant state at the Fermi energy due to the admixture of the electronically active and highly local f orbitals with the metallic band of the host. Heavy fermions are usually modeled by the single impurity Anderson model or the periodic Anderson model depending on the concentration of the correlated f orbitals.

Photoemission experiments provide a direct probe of the characteristic resonant states in these materials. However, there are two apparently contradictory sets of photoemission results. The large body of spectroscopic data accumulated by the Bell Lab and Neuchatel groups for scraped polycrystalline samples consistently indicate qualitative and sometimes quantitative agreement with the predictions of the single impurity models [2]. On the other hand some recent photoemission results obtained by the Los Alamos group for single-crystalline samples cleaved *in situ* have revealed several apparent inconsistencies with the predictions of single impurity models, including enhanced intensity, a much weaker temperature dependence and a dispersion of the Kondo peak [3]. This has caused a persistent dispute regarding the ability of single impurity models to describe the observed resonant state in Kondo materials [4]. We refer the reader to Malterre *et al.* [5] for a recent review.

The single impurity Anderson model (SIAM) is typically used as the paradigm for comparison with experiments due to its universality, the abundance of good approximations, and the existence of exact solutions. Although at high temperatures the SIAM captures the same physics as the lattice model, it cannot account for the electronic coherence at low temperatures. The periodic

Anderson model (PAM) is believed to correctly describe the strong correlation of f electrons as well as their coherence at low temperatures and the interaction between the screened moments.

We have recently analyzed some static properties of the PAM [6]. We found that when the f band filling $n_f \approx 1$ and the d band filling $n_d \lesssim 0.8$ (so that the system is metallic), the Kondo scale for the PAM, T_0 , is strongly suppressed compared to T_0^{SIAM} , the Kondo scale for a SIAM with the same model parameters. However the high temperature ($T > T_0^{SIAM}$) properties of the two models are similar, so that T_0^{SIAM} is also the relevant scale for the onset of screening in the PAM whereas T_0 is the scale for the onset of coherence. We found no universal relation between T_0^{SIAM} and T_0 (their ratio depends on the d band filling). We also demonstrated that in the screening regime ($T \lesssim T_0^{SIAM}$) the rate of change of the local magnetic moment with temperature is smaller in the PAM than in the SIAM.

In this paper we show that the PAM predicts a much weaker temperature dependence for the Kondo peak than the SIAM, consistent with the experiments on single-crystalline Kondo lattice materials. We also show that the Kondo peak is dispersive in the PAM, giving rise to heavy quasiparticle bands near the Fermi energy. We use Nozieres' idea of the effective Hubbard model for the screening clouds [7] to interpret this "band formation" and the slow evolution of the Kondo peak. This also gives insight into the emergence of two relevant energy scales (T_0^{SIAM} and T_0) in the PAM.

Method The PAM Hamiltonian on a D -dimensional hypercubic lattice is,

$$\begin{aligned}
 H = & \frac{-t^*}{2\sqrt{D}} \sum_{\langle ij \rangle \sigma} \left(d_{i\sigma}^\dagger d_{j\sigma} + \text{H.c.} \right) \\
 & + \sum_{i\sigma} \left(\epsilon_d d_{i\sigma}^\dagger d_{i\sigma} + \epsilon_f f_{i\sigma}^\dagger f_{i\sigma} \right) + V \sum_{i\sigma} \left(d_{i\sigma}^\dagger f_{i\sigma} + \text{H.c.} \right) \\
 & + \sum_i U (n_{f i \uparrow} - 1/2)(n_{f i \downarrow} - 1/2) . \quad (1)
 \end{aligned}$$

In Eq. (1), $d(f)_{i\sigma}^{(\dagger)}$ destroys (creates) a $d(f)$ electron with spin σ on site i . The hopping is restricted to the nearest neighbors and scaled as $t = t^*/2\sqrt{D}$. U is the screened on-site Coulomb repulsion for the localized f states and V is the hybridization between d and f states. This model retains the features of the impurity problem, including moment formation and screening, but is further complicated by the lattice effects.

Metzner and Vollhardt [8] observed that the irreducible self-energy and vertex-functions become purely local as the coordination number of the lattice increases. As a consequence, the solution of an interacting lattice model in $D = \infty$ may be mapped onto the solution of a local correlated impurity coupled to a self-consistently determined host [9]. We employ the quantum Monte Carlo (QMC) algorithm of Hirsch and Fye [10] to solve the remaining impurity problem and calculate the imaginary time local Green's functions. We then use the maximum entropy method [11] to find the f and d density of states and the self-energy [12].

Results We simulated the PAM for a wide variety of fillings and parameters in units of t^* (considered to be a few electron-volts, the typical band-width of conduction electrons in metals). Here we present the results for $U = 1.5$, $V = 0.6$, $n_f \approx 1$ with two different d band fillings $n_d = 0.4$ and $n_d = 0.6$ for which the Kondo scales are $T_0 = 0.014$ and $T_0 = 0.054$ respectively. We use the symmetric limit of the SIAM ($n_f = n_d = 1$) for the comparison since the results for the SIAM are universal and hence independent of the filling.

Fig. 1 shows the f density of states for the PAM and SIAM near the Fermi energy $E_F = 0$. Both models show temperature-dependent Kondo peaks of similar width, but the rate of change of the peak intensity with temperature is much smaller and the Kondo peak persists up to much higher temperatures in the PAM than for the SIAM. This is consistent with the protracted behavior of screened moments in the PAM [6], i.e., the rate of change of the screened moments with temperature is much smaller in the PAM compared to the SIAM when $n_d \lesssim 0.8$ and $n_f \approx 1$. Note the difference in scales of the two parts of this figure, both the intensity and the spectral weight of the Kondo peak are larger in the PAM than in the SIAM although the hybridization parameter V is larger for the PAM in this case. This shows (and we generally find) that the height of the Kondo peak in the PAM does not scale like $1/V^2$ as it does in the impurity models. For the PAM, starting at high temperatures the Kondo resonance peak is located well above the Fermi energy but as we lower the temperature it shifts toward E_F . Hence there is a spectral weight transfer into the region around the Fermi energy as the temperature is lowered but we can see that the spectral weight in this region increases slower in the PAM than in the SIAM.

Fig. 2 shows the momentum dependence of the f and d

spectral functions for the PAM along the diagonal direction of the Brillouin zone (the main conclusions do not depend on the chosen direction). In the large- D hypercubic lattice, the zone center (corner) corresponds to a very large negative (positive) ϵ_k . We see that near the zone center (lowest part of the figure) there are two apparent maxima, the lower one has mostly d character the upper one mostly f character. The latter has a narrow Kondo like feature but would not be seen in photoemission experiment since it is located above the Fermi energy. The quasiparticle peak (Kondo peak) near the Fermi surface starts to develop only as \mathbf{k} moves well away from the zone center. Note that there is a gradual transformation of this peak from a mixed fd -character at $\epsilon_k = 0$ to an almost entirely f character at and above $\epsilon_k = 1.23$. In addition to these narrow peaks the data shows a small and broad non-dispersive peak near $\omega = -0.8$ which has mostly f character. This is a remnant of the lower unhybridized f level, we were not able to resolve the peak corresponding to the upper f level for these model parameters (we resolve this peak if we use a larger value for U/V^2).

We clarify this situation in Fig. 3. The symbols in this figure show the position of f and d spectral functions maxima versus ϵ_k and the solid line shows the quasiparticle energy, calculated from the real part of the pole of the Green's functions. In the narrow region above the Fermi surface we see an almost dispersionless band. The imaginary part of these poles are very large, so they correspond to very broad peaks in the spectral functions which we were not able to resolve. The bands above and below this region correspond to well defined peaks in the spectral functions. The general features of this band structure for the PAM persists up to very high temperatures ($T/T_0 \gtrsim 10$).

The imaginary part of self-energy has a maximum near the Fermi energy (not shown); its position shifts toward E_F and its value approaches zero as the temperature is lowered. This suggests a Fermi-liquid like behavior for the model. Furthermore, the real part of the effective self-energy for the d electrons shows a large negative slope near the Fermi energy which denotes a large effective mass for the d electrons. We can use the self-energy to calculate the optical conductivity and the dc resistivity of the model (the details of calculations will appear in a future publication). At temperatures of the order of T_0^{SIAM} the resistivity shows a log-linear behavior adjacent to a maximum, just like what is expected from a Kondo-type resistivity for a dilute system. As the temperature is lowered toward T_0 the resistivity flattens. Below T_0 the resistivity decreases quickly towards zero indicating the onset of coherence and the emergence of a Fermi-liquid (metallic) behavior.

Interpretation Some of these results are consistent with a simple band-formation picture. When $V = 0$ the available electronic states consist of a d band and

two (doubly degenerate) local f levels separated by U . When V is turned on, a new resonant state forms near the Fermi surface. Furthermore, the original d band mixes with the local f levels and the resonant level, giving rise to a renormalized band which has f character near the renormalized f level energies and has d character far from them as we see in Fig. 3. The Kondo states near E_F have mostly f character indicating that the f electrons themselves are involved in screening the local moments through hybridization with the d band. This is like the situation in a single-band Hubbard model, where the electrons within the band are responsible for screening the “local moments” in that band.

We can understand the emergence of the two energy scales (T_0^{SIAM} and T_0) and the protracted screening of the moments in the PAM using the arguments of Noziers [7]. He argued that since the screening cloud of a local magnetic moment involves conduction electrons within T_0^{SIAM}/T_F of the Fermi surface, only a fraction of the moments $n_{eff} \approx N_d(0)T_0^{SIAM}$ may be screened by the conventional Kondo effect. He then proposed that the screened and unscreened sites may be mapped onto particles and holes of an effective Hubbard model with local Coulomb repulsion U . The screening clouds hop from site to site and effectively screen all the moments in a dynamical fashion. The hopping constant of this effective model is strongly suppressed relative to t^* by the overlap of the screened and unscreened states. Thus the Kondo scale of the effective model becomes much less than T_0^{SIAM} . This leads to the protracted screening behavior which is a crossover between the two regimes of Kondo screening at the higher scale T_0^{SIAM} and coherent screening at the lower scale T_0 . In this argument the two scales depend on n_{eff} and hence there can be no universal relation between them.

Comparison with experiment For the purpose of comparison with experiment we focus our attention on the data for CeBe₁₃ compound because it has a large enough Kondo temperature that current high resolution apparatus should be able to probe its Kondo resonant state. CeBe₁₃ is a mixed-valent heavy fermion compound with a small number of conduction electrons per site and a rather large Kondo temperature ($T_K \approx 400K$) so the PAM with the parameters we chose for $n_d = 0.4$ is suitable for comparison with experimental observations on this material ($T_0 \approx 320K$ if $t^* \approx 2eV$). A series of photoemission experiments on single crystalline samples of Ce compounds including CeBe₁₃ have suggested a temperature dependence for the Kondo peak which is much weaker than what one expects from single-impurity model calculations [3], this is consistent with Fig. 1.

Photoemission spectra obtained by choosing various incident angles on CeBe₁₃ crystals have shown a dispersive structure near the Fermi surface which is persistent up to temperatures of the order of $10T_K$ [15]. As we showed in Fig. 1 the PAM predicts a Kondo peak at these

higher temperatures whereas the SIAM does not. Our results also show the dispersive nature of the quasiparticles as shown in Fig. 3. The photoemission observations show that the quasiparticle peak intensity near E_F is a minimum at the zone center and tends to develop as \mathbf{k} deviates from the zone center and reaches its highest value at the zone corner. This is consistent with what we see in Fig. 2.

Conclusions We find that in the metallic regime where $n_d \lesssim 0.8$ and $n_f \approx 1$: i) The PAM predicts a Kondo peak which has a weaker temperature dependence and persists up to much higher temperatures (in units of the Kondo scale) compared to the predictions of the SIAM. ii) Both the intensity and the spectral weight of the Kondo peak are larger in the PAM than in the SIAM. iii) The Kondo peak intensity does not scale like $1/V^2$ in the PAM. iv) The Kondo peak is dispersive in the PAM making a heavy quasiparticle band which crosses the Fermi surface. This can be interpreted as the heavy band emerging from an effective Hubbard model for the local screening clouds introduced by Noziers. v) The Kondo peak below the Fermi energy starts to develop only as \mathbf{k} deviates from the zone center, consistent with experiment. vi) There are two relevant energy scales for the PAM: the onset of screening scale T_0^{SIAM} , and the onset of coherence scale T_0 which is strongly suppressed compared to the latter. This is also consistent with Noziers arguments.

These results provide a consistent interpretation of the Los Alamos photoemission experiments involving single-crystals, but not the results of the Bell Labs and Neuchâtel groups involving poly-crystals. Thus, a controversy persists. However, we note that near the insulating regime ($n_d \approx n_f \approx 1$) both the PAM Kondo scale (T_0) and screening rate are enhanced compared to those of the SIAM and Noziers’ arguments do not apply. In the narrow region where the system is doped away from the insulating state, both the screened local moment and the spectra show impurity-like temperature dependence. It is possible that this, or a more realistic model, including the effects of disorder, orbital degeneracy, or crystal field effects may provide a unifying interpretation of all of the photoemission spectra.

We would like to acknowledge stimulating conversations with J. Allen, A. Arko, A. Chattopadhyay, D.L. Cox, B. Goodman, M. Grioni, D.W. Hess, M. Hettler, J. Joyce, H.R. Krishnamurthy, Th. Pruschke, P. van Dongen and F.C. Zhang.

Jarrell and Tahvildar-Zadeh would like to acknowledge the support of NSF grants DMR-9704021 and DMR-9357199. Freericks acknowledges the support of an ONR-YIP grant N000149610828. Tahvildar-Zadeh and Freericks received partial support from the Petroleum Research Fund, administered by the American Chemical Society (ACS-PRF 29623-GB6). Computer support was provided by the Ohio Supercomputer Center.

- [1] For a review see D.W. Hess, P.S. Riseborough and J.L. Smith, *Enc. of Applied Physics* edited by G. L. Trigg (VCH Publishers Inc., New York, 1991), Vol. 7, p. 435; and N. Grewe and F. Steglich, *Handbook on the Physics and Chemistry of Rare Earths*, edited by K.A. Gschneidner, Jr. and L.L. Eyring (Elsevier, Amsterdam, 1991), Vol. 14, p. 343.
- [2] L.H. Tjeng *et al.*, Phys. Rev. Lett. **71**, 1419 (1993), see also M. Garnier *et al.*, Phys. Rev. Lett. **78**, 4127 (1997)
- [3] J.J. Joyce *et al.*, Phys. Rev. Lett. **68**, 236 (1992).
- [4] For example see J.J. Joyce *et al.*, Phys. Rev. Lett. **72**, 1774 (1994); and L.H. Tjeng *et al.*, Phys. Rev. Lett. **72**, 1775 (1994).
- [5] D. Malterre *et al.*, Adv. in Phys. **45**, 299, (1996).
- [6] A.N. Tahvildar-Zadeh, M. Jarrell and J.K. Freericks, Phys. Rev. **B55**, R3332 (1997).
- [7] P. Nozieres, Ann. Phys. Fr. **10**, 19-35 (1985).
- [8] W. Metzner and D. Vollhardt, Phys. Rev. Lett. **62**, 324 (1989); see also E. Müller-Hartmann, Z. Phys. B **74**, 507 (1989).
- [9] Th. Pruschke, M. Jarrell and J.K. Freericks, Adv. in Phys. **42**, 187 (1995), and A. Georges, G. Kotliar, W. Krauth, and M. Rozenberg, Rev. Mod. Phys. **68**, 13 (1996).
- [10] J.E. Hirsch and R.M. Fye, Phys. Rev. Lett. **56**, 2521 (1989).
- [11] M. Jarrell and J.E. Gubernatis, Physics Reports Vol. **269** No.3, p133-195, (May, 1996).
- [12] M. Jarrell, Phys. Rev. B, **51**, 7429 (1995).
- [13] H. Schweitzer and G. Czycholl, Z. Phys. B - Condensed Matter **79**, 377-388 (1990).
- [14] A. N. Tahvildar-Zadeh, M. Jarrell and J.K. Freericks, In preparation.
- [15] A. B. Andrews *et al.*, Phys. Rev. **B53**, 3317 (1996).

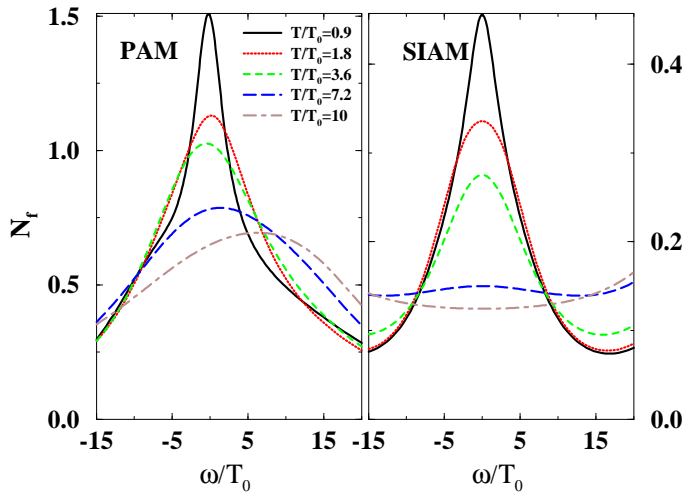


FIG. 1. Near-Fermi-energy ($E_F = 0$) structure of the f density of states for the asymmetric PAM (left) and the symmetric SIAM (right). The model parameters are $U = 1.5$, $V = 0.6$, $n_d = 0.4$ for the PAM and $U = 2.75$, $V = 0.5$, $n_d = 1.0$ for the SIAM. The temperature dependence of the peak is universal for the SIAM and hence independent of the band fillings. Note that T_0 refers to the two different Kondo scales of the PAM (left) and the SIAM (right).

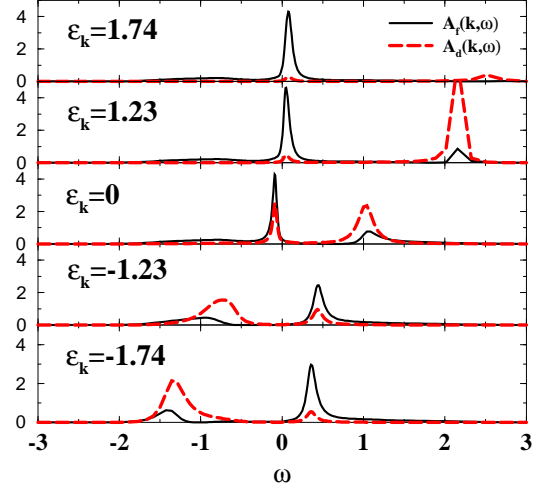


FIG. 2. The PAM f and d spectral functions for different values of the momentum vector \mathbf{k} for $U = 1.5$, $V = 0.6$, $n_f \approx 1.0$, $n_d = 0.6$ and $T/T_0 = 0.46$. ϵ_k is the unrenormalized band energy. The Fermi energy is located at $\omega = 0$.

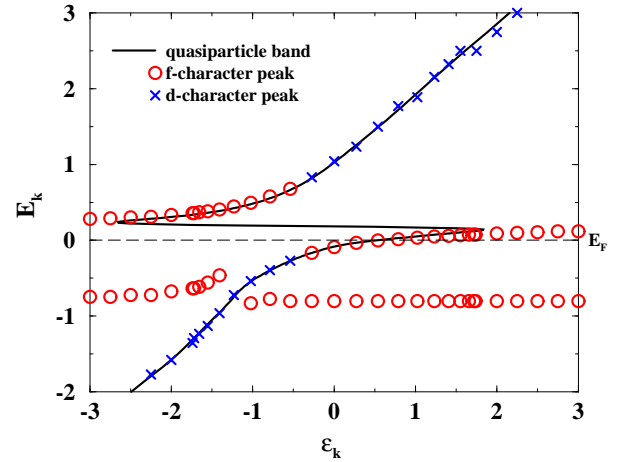


FIG. 3. Band structure for the PAM. The model parameters are the same as in Fig. 2. However the features persist up to $T/T_0 \approx 10$. The solid line shows the real part of the Green's functions poles vs. ϵ_k the unrenormalized band energy. The symbols show the positions of the maxima in the f and d spectral functions. We characterize these peaks to be of f character whenever $A_f(\epsilon_k, E_k) > A_d(\epsilon_k, E_k)$ or d character whenever $A_f(\epsilon_k, E_k) < A_d(\epsilon_k, E_k)$ (cf. Fig. 2).